Heritability analysis with repeat measurements and its application to resting-state functional connectivity

Tian Ge[a,b,c,1], Avram J. Holmes[a,d,e], Randy L. Buckner[a,e,f,g], Jordan W. Smoller[b,c,2], and Mert R. Sabuncu[a,h,i,1,2]

[a]Athinoula A. Martinos Center for Biomedical Imaging, Massachusetts General Hospital, Harvard Medical School, Charlestown, MA 02129; [b]Psychiatric and Neurodevelopmental Genetics Unit, Center for Genomic Medicine, Massachusetts General Hospital, Boston, MA 02114; [c]Stanley Center for Psychiatric Research, Broad Institute of MIT and Harvard, Cambridge, MA 02138; [d]Department of Psychology, Yale University, New Haven, CT 06520; [e]Department of Psychiatry, Massachusetts General Hospital, Harvard Medical School, Boston, MA 02114; [f]Department of Psychology, Harvard University, Cambridge, MA 02138; [g]Center for Brain Science, Harvard University, Cambridge, MA 02138; [h]School of Electrical and Computer Engineering, Cornell University, Ithaca, NY 14853; and [i]Nancy E. and Peter C. Meinig School of Biomedical Engineering, Cornell University, Ithaca, NY 14853

Edited by Marcus E. Raichle, Washington University in St. Louis, St. Louis, MO, and approved April 12, 2017 (received for review January 17, 2017)

Heritability, defined as the proportion of phenotypic variation attributable to genetic variation, provides important information about the genetic basis of a trait. Existing heritability analysis methods do not discriminate between stable effects (e.g., due to the subject's unique environment) and transient effects, such as measurement error. This can lead to misleading assessments, particularly when comparing the heritability of traits that exhibit different levels of reliability. Here, we present a linear mixed effects model to conduct heritability analyses that explicitly accounts for intrasubject fluctuations (e.g., due to measurement noise or biological transients) using repeat measurements. We apply the proposed strategy to the analysis of resting-state fMRI measurements—a prototypic data modality that exhibits variable levels of test–retest reliability across space. Our results reveal that the stable components of functional connectivity within and across well-established large-scale brain networks can be considerably heritable. Furthermore, we demonstrate that dissociating intra- and intersubject variation can reveal genetic influence on a phenotype that is not fully captured by conventional heritability analyses.

heritability | repeat measurements | resting-state fMRI | functional connectivity | test–retest reliability

Heritability is defined as the proportion of phenotypic variation that can be explained by genetic variation among individuals in a population (1). It is a fundamental concept in population and statistical genetics, providing basic but important information about the genetic underpinnings of a trait. The heritability of a large number of human complex traits across a wide range of the phenotypic spectrum has been documented, using classical twin or pedigree designs (2–4), or statistical methodologies developed more recently that allow for the estimation of heritability in large samples of unrelated individuals (5–9).

Statistical models for heritability analysis typically include an error term (residual) that absorbs the phenotypic variation that cannot be explained by genetics and common environment. The residual therefore accounts for unique (subject-specific) environmental effects, measurement error, and intrasubject fluctuation of the trait due to, for example, biological cycles such as the circadian rhythm. With one measurement for each subject, these factors cannot be dissociated and are typically modeled jointly as an independent and identically distributed random variable across subjects. However, this model imposes at least two problems on heritability analysis. First, measurement error has a ceiling effect on heritability estimates; it inflates the total phenotypic variation and downwardly biases heritability estimates. Second, comparing the heritability of traits that have different levels of measurement noise may be misleading.

The issues can be partially resolved if repeat measurements of a trait are available. Assuming that multiple repeat measurements have been collected for each subject over a period in which we expect little biologically meaningful change to the trait (i.e., the genetic architecture of the trait and the environmental influences remain largely unchanged during the time period), we can then distinguish factors that contribute to the intersubject variation of the phenotype but are stable across repeat measurements (e.g., due to unique environmental effects) from factors that exhibit intrasubject fluctuation (e.g., measurement error). Defining heritability as the fraction of the total stable intersubject variation that is attributable to genetic variation removes the ceiling effect of measurement error and makes the heritability estimates of traits that have different levels of noise comparable. To date, however, repeat measurements have rarely been used this way in heritability estimation. Instead, serial measurements are typically averaged, yielding one scalar measurement for each subject such that conventional heritability analysis methods can be applied. Although averaging repeat measurements cancels out some measurement error and thus improves the reliability of the phenotype, it does not dissociate intra- and intersubject variation and can still lead to the underestimation of the heritability of a trait in the presence of noise and biological transients.

In this paper, we present a linear mixed effects (LME) model that can leverage repeat measurements to explicitly dissociate intra- and intersubject variation of a phenotype and compute heritability with respect to stable intersubject variation. As a demonstration of application, we investigate the heritability of (intrinsic) functional connectivity measurements derived from resting-state fMRI (rs-fMRI). rs-fMRI is a prototype case with a substantial amount of measurement noise from multiple

Significance

Heritability is a fundamental metric in population genetics. Existing heritability models lump together stable effects (e.g., due to the subject's unique environment) and transient effects, such as measurement error. This can result in misleading assessments when comparing the heritability of traits that exhibit different levels of reliability. This paper presents a heritability estimation strategy that can account for transient intrasubject variation using repeat measurements. Using the proposed method, we show that the stable components of functional connectivity within and across well-established large-scale brain networks can be considerably heritable. With the explosive expansion of genomics, health informatics, and digital phenotyping technologies, the proposed model will be significant in dissecting the genetic basis of a wide range of informative but noisy phenotypes.

Author contributions: T.G., R.L.B., J.W.S., and M.R.S. designed research; T.G. and A.J.H. performed research; T.G. and M.R.S. contributed new reagents/analytic tools; T.G. and A.J.H. analyzed data; and T.G., A.J.H., R.L.B., J.W.S., and M.R.S. wrote the paper.

The authors declare no conflict of interest.

This article is a PNAS Direct Submission.

[1]To whom correspondence may be addressed. Email: tge1@mgh.harvard.edu or msabuncu@nmr.mgh.harvard.edu.

[2]J.W.S. and M.R.S. contributed equally to this work.

This article contains supporting information online at www.pnas.org/lookup/suppl/doi:10.1073/pnas.1700765114/-/DCSupplemental.

NEUROSCIENCE

sources (including thermal, system, and physiological) (10, 11). Long-range functional connectivity computed from rs-fMRI time series might span distant brain regions that have dramatically different levels of measurement error due to the complex spatial pattern of the noise and susceptibility artifacts. Moreover, the brain is a dynamic system where time-varying fluctuations in functional connectivity and brain networks and transitions between different brain states have been observed (12). Therefore, part of the variation in rs-fMRI–derived measurements can be attributed to a nontransient component for each subject, and another portion of the variation might be due to transient neuronal activity or other factors that influence coupling between regions and can change between scanning sessions of a subject.

Recent studies have also shown that individual differences in functional connectivity are heterogeneous across the cortex after accounting for intrasubject variation, with greater variability in high-level association cortex (e.g., prefrontal cortex and the inferior parietal lobule) and lesser variability in unimodal regions (e.g., visual cortex and somatosensory cortex), pointing to a potential relationship between the spatial distribution of intersubject variation in functional connectivity and brain evolution and development (13). Disentangling the nontransient, stable component of rs-fMRI measurements from the transient signal across repeat scans and estimating the stable heritability might thus improve our understanding of the genetic basis of brain function.

Although a handful of studies have investigated the genetic basis of the functional connectome and functional brain networks (14–16), to our knowledge none has addressed intra- and intersubject variation of rs-fMRI measurements, despite the fact that repeat scans are commonly collected in rs-fMRI studies. Here, using rs-fMRI data collected by the Human Connectome Project (HCP) (17) and the Harvard/Massachusetts General Hospital (MGH) Brain Genomics Superstruct Project (GSP) (18, 19), we demonstrate that (*i*) the relative contributions of intra- and intersubject variation to the total variation of rs-fMRI–derived functional connectivity measurements are dramatically different across space and strongly correlated with test–retest reliability, (*ii*) the stable component of functional connectivity (within and between well-established large-scale functional brain networks) can be substantially heritable, and (*iii*) dissociation of intra- and intersubject variation can reveal genetic influences on the functional architecture of the human brain that are not detectable by conventional heritability analyses. Our results provide insights into the genetic basis of brain function and highlight the importance of accounting for the spatial pattern of measurement noise and transient signals when studying the heritability of functional connectivity measurements across brain regions.

Results

We first conducted simulation studies to ensure that the proposed LME model can robustly dissociate intra- and intersubject variation of a phenotype and accurately estimate heritability due to intersubject variation using repeat measurements (*Supporting Information*). As shown in Fig. S1, the proposed method consistently produced unbiased estimates, whereas results obtained with the classical model were affected by intrasubject variation.

Next, we sought to characterize the spatial distribution of intra- and intersubject variation of functional connectivity measurements using real rs-fMRI data. Specifically, we analyzed 582 young and healthy subjects (92 monozygotic twin pairs, 46 dizygotic twin pairs, 250 full siblings, and 56 singletons) from the HCP and 809 unrelated young and healthy subjects from the GSP. A previously published and widely validated rs-fMRI–based parcellation of seven cortical functional networks (visual, somatomotor, dorsal attention, ventral attention/salience, limbic, control, and default network) (18) was split into 51 spatially contiguous regions across the two hemispheres (Fig. 1*A*). For each rs-fMRI scan, spatially normalized Pearson correlation coefficients between preprocessed time series at pairs of cortical locations were summarized within and across these network regions into a 51×51 matrix. When averaging across subjects, the functional connectivity matrices computed from both the HCP and GSP sample showed clear modular structures (Fig. 1*B*). In particular, negative correlations between attention networks and the default mode network (DMN) can be clearly observed.

We fit the proposed LME model that partitions the total phenotypic variation into intersubject variation (the stable, nontransient component) and intrasubject variation (including the unstable, transient component and measurement error), using the 51×51 functional connectivity matrices computed for each rs-fMRI session in the HCP sample. Fig. 2*A* shows that the relative contributions of intra- and intersubject variation are highly heterogeneous across space. The spatial pattern of intersubject variation is similar to and highly correlated with (Pearson's $r = 0.845$) the test–retest reliability of functional connectivity measurements estimated using a subset of the HCP subjects that were sampled from different families and had repeat rs-fMRI scans (Fig. 2 *B* and *C*, *Left*). The intersubject variation estimated in HCP also agrees with the test–retest reliability of functional connectivity measurements estimated using the independent GSP sample (Pearson's $r = 0.548$; Fig. 2 *B* and *C*, *Right*). Within-network functional connectivity shows larger intersubject variation and higher test–retest reliability than between-network connectivity in general. Yet, there are certain exceptions, such as the connectivity between the control and default network, which is also highly reliable. There is strong agreement between the spatial patterns of test–retest reliability estimated using the HCP and GSP.

The heritability of the stable, nontransient component of rs-fMRI–derived functional connectivity measurements, defined as the proportion of intersubject variation attributable to the genetic variation in the population, is substantial for many pairs of brain regions (Fig. 3, *Right*) and is consistently higher than conventional heritability estimates (the proportion of the total phenotypic variation attributable to genetic variation; Fig. 3, *Left*) computed by averaging repeat measurements for each individual and applying the classical ACE model (A, additive genetics; C, common environment; E, unique environment). Overall, within-network functional connectivity measurements for all of the seven functional networks are significantly heritable, but the nontransient heritability estimates are consistently larger than the conventional heritability estimates (Fig. 3*B*).

Finally, we conducted an analysis of the functional connectivity profile seeded in the posterior cingulate cortex (PCC), a core region of the DMN, in the HCP sample. The PCC is strongly positively correlated with other regions in the DMN such as the medial prefrontal cortex, inferior parietal lobule, and lateral temporal cortex, and negatively correlated with the dorsal and ventral attention networks (Fig. 4*A*). Functional connectivity within the DMN shows high test–retest reliability and low intrasubject variation, whereas regions not coupled with the PCC such as the motor and somatosensory cortex and visual cortex show lower test–retest reliability and higher intrasubject variation (Fig. 4 *B* and *F*). The heritability maps of the functional connectivity profile estimated by the classical ACE model (Fig. 4*C*) and the proposed LME model (Fig. 4*D*) have similar patterns in general; both clearly show that functional connectivity within the DMN is highly heritable. Contrasting the two heritability maps reveals that the proposed LME method produces substantially higher heritability estimates than the classical ACE model in the attention networks and the visual cortex (Fig. 4*E*), indicating that the functional connectivity between PCC and these regions might be under strong genetic influence after accounting for the unstable, transient signal in functional connectivity measurements.

Discussion

In this paper we presented an LME model that can explicitly dissociate stable, nontransient intersubject variation (e.g., due to long-lasting unique environmental effects) and transient, intrasubject measurement-to-measurement variation (e.g., due to measurement noise and state-varying factors) of a phenotype using repeat measurements. By defining nontransient heritability

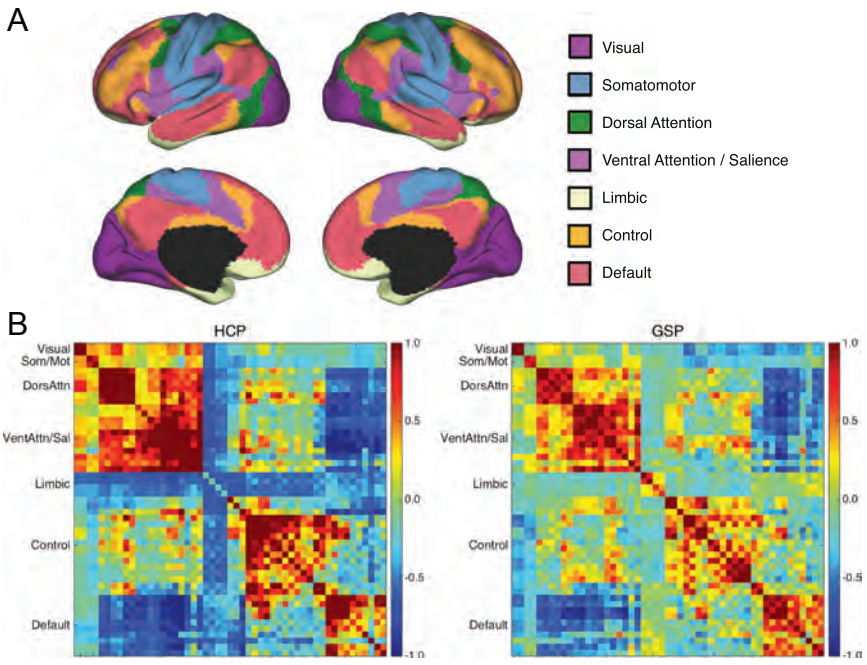

Fig. 1. Functional connectivity measurements between pairs of 51 brain regions. (*A*) Surface representation of the seven-network parcellation (18), which can be split into 51 spatially contiguous regions across the two hemispheres. (*B*) Average functional connectivity measurements between pairs of the 51 brain regions across subjects in the HCP sample (*Left*) and GSP sample (*Right*).

as the proportion of the stable intersubject variation that can be explained by genetic variation, we can correct for the effect of intrasubject fluctuations on heritability estimates and put phenotypes with different levels of measurement noise on equal footing to assess their comparative heritability.

The proposed statistical model is an extension to the classical LME model for longitudinal data with a random intercept (20, 21), which is used in a wide range of fields to account for intra- and intersubject variation in repeat measurements. Incorporating genetic and environmental effects into the model naturally introduces a covariance structure across subjects, in contrast to assuming independent samples in conventional longitudinal data analysis. The proposed model can also be viewed as an extension to the classical ACE model, which is widely used in heritability analysis. Specifically, in addition to the genetic and environmental factors, a random effect that captures intrasubject variation is included. With repeat measurements, all random effects in the model have different covariance structures and thus the model is identifiable and can be fitted using the restricted maximum likelihood (ReML) estimation (22). Similar attempts to correct for measurement error in heritability analysis with repeat measurements have been made in twin studies using structural equation modeling (23, 24). Although we demonstrated our method using an extended twin sample collected by the HCP, the model can be easily applied to heritability analysis in unrelated individuals, where the genetic similarity matrix is empirically estimated from genome-wide SNPs (5, 6).

The proposed method can be applied to any phenotype on which repeat measurements are available. In particular, with the recent convergence of imaging, genomics, health informatics, and digital phenotyping technologies, the model has the potential to dissect the genetic basis of a wide range of novel, informative, but noisy phenotypes on which repeat measurements can be collected, such as gene expression, wearable sensor data, and web-based cognitive and behavioral assessments. We have used functional connectivity measurements computed from rs-fMRI as an example because repeat scans are often collected in fMRI studies, and it is known that rs-fMRI features often contain a substantial amount of noise from multiple sources and typically have lower test–retest reliability than morphological measurements derived from structural brain MRI scans. We confirmed that for some functional connectivity more than 70% of the phenotypic variation can be attributed to transient intrasubject variation. More importantly, the contribution of the stable, nontransient component of functional connectivity to the total phenotypic variation varies dramatically across space and is strongly correlated with the test–retest reliability of the measurements. For example, connectivity measurements between the limbic network (e.g., the temporal pole and orbitofrontal regions) and other brain regions have much smaller stable intersubject components and relatively lower test–retest reliability (19), likely due to susceptibility artifacts associated with sinus and temporal bone regions (25, 26). Head motion might also have systematic influences on rs-fMRI–derived measurements and exert differential effects on distant and regional functional couplings (27–29). The heterogeneous distribution of the spatial noise and confounds in rs-fMRI underscores the importance of accounting and correcting for intrasubject variation when comparing the heritability of functional connectivity measurements across space. Although the reliability of rs-fMRI signals depends on the scanner type and imaging sequence, we observed largely consistent spatial patterns of test–retest reliability between the HCP and GSP samples, suggesting that a large portion of the measurement-to-measurement variation might be dominated by factors shared across imaging sites, scanning protocols, and samples.

Previous studies have shown that resting-state functional connectivity measurements within the DMN are significantly heritable (14). Graph theoretical measures that index topological characteristics and communication efficiency of intrinsic brain networks were also found to be heritable in both adults (15) and normally developing children (30). We have demonstrated in the present study that the stable, nontransient components of rs-fMRI–derived functional connectivity measurements are highly heritable between many brain regions, and all functional networks we examined have substantially heritable within-network couplings. The heritability analysis of the functional connectivity profile seeded in the PCC, a core region of the DMN (31), further confirmed that the intrinsic connectivity of

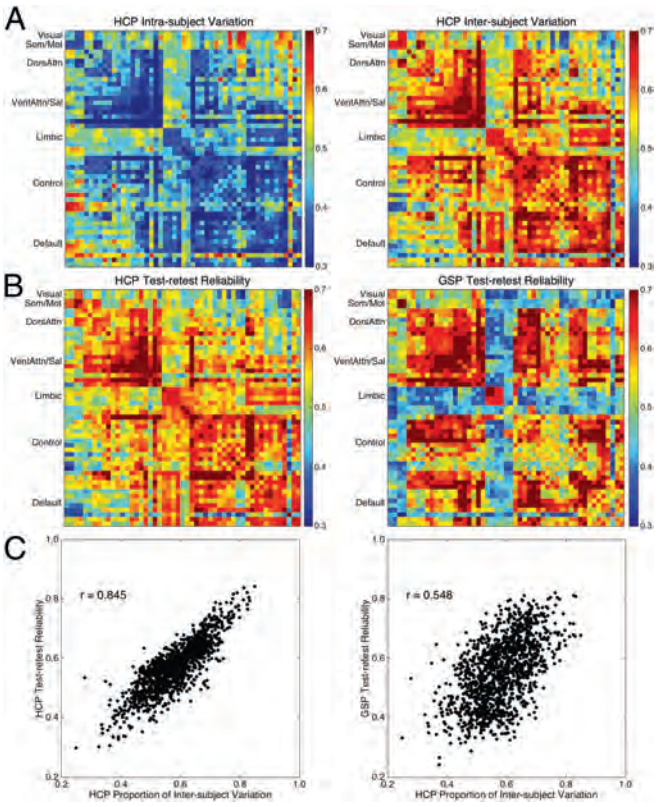

Fig. 2. Intra- and intersubject variation of the resting-state functional connectivity measurements. (*A*) Proportion of the total phenotypic variation attributable to intrasubject measurement-to-measurement variation (*Left*) and stable, nontransient intersubject variation (*Right*) estimated in the HCP sample. (*B*) Test–retest reliability of the functional connectivity measurements estimated using the HCP sample (*Left*) and GSP sample (*Right*). (*C*) Test–retest reliability of the functional connectivity measurements estimated in the HCP (*Left*) and GSP (*Right*) plotted against the proportion of phenotypic variance explained by the intersubject variation estimated in the HCP sample.

large-scale brain networks is under strong genetic influence. Moreover, using the proposed LME model, we identified that several regions that are weakly correlated (e.g., the visual cortex) or negatively correlated with PCC (e.g., the attention networks) exhibit highly heritable nontransient functional couplings with the seed. This is in contrast with the picture offered by a conventional heritability analysis, in which heritability estimates of these weak or negative couplings did not stand out from the background, likely because these regions are not consistently coactivated across subjects during rest, and the associated functional connectivity measurements comprise large transient components that vary from scan to scan. Our analyses provide heritability estimates of functional connectivity for multiple brain networks. Our results indicate that the proposed method has the potential to unveil the genetic basis of the functional connectome that cannot be fully captured by conventional heritability analyses.

There are some technical limitations of the proposed method. First, we note that although nontransient heritability estimates defined with respect to stable intersubject variation are typically larger than conventional heritability estimates, the statistical power (in terms of testing the significance of heritability) will not necessarily be larger because the proposed model includes one more parameter than the ACE model and thus the uncertainties in the point estimates of variance component parameters might increase. In fact, there may be a substantial power loss when applying the proposed model in a setting of moderate sample size, small number of repeat measurements, and large measurement error. In this case, the classical model is recommended for more robust model fitting and statistical inferences. Second, the proposed method cannot distinguish artifacts that are correlated with variables of interest (e.g., genetic and environmental factors) and/or manifest as stable intersubject variation (e.g., anatomical variability that contributes to functional connectivity estimates). More sophisticated models or better preprocessing techniques are needed to identify and remove this type of noise and anatomical confound. Finally, it is important to emphasize that the proposed model merely examines stable intersubject phenotypic variation, while treating temporal variation as a nuisance. Future work is needed to extend the proposed strategy to longitudinal settings, such as during development or progressive disease, where the temporal dynamics of a measurement is the phenotype of interest.

Methods

The Model. We consider the following LME model for repeat measurements (20, 21):

$$y_{ij} = \boldsymbol{x}_{ij}^{\top}\boldsymbol{\beta} + \gamma_i + \epsilon_{ij}, \quad i = 1, 2, \cdots, m, \quad j = 1, 2, \cdots, n_i, \qquad [1]$$

where m is the total number of subjects; y_{ij} is the j-th repeat measurement from the i-th subject, and the number of repeat measurements n_i can be subject-specific; $\boldsymbol{x}_{ij}$ is a $q \times 1$ vector of covariates such as age and sex; $\boldsymbol{\beta}$ is a $q \times 1$ vector of unknown fixed (population-level) effects; γ_i is a random intercept, which describes subject-specific deviation from the population mean; and ϵ_{ij} denotes intrasubject measurement-to-measurement variation (e.g., measurement error or the unstable, transient component) of y_{ij} and is assumed to be independent of the random effects and independent between repeat measurements. We assume that $\boldsymbol{\gamma} = [\gamma_1, \cdots, \gamma_m]^{\top}$ can be partitioned into the sum of additive genetic effect $\boldsymbol{g}$, common (or shared) environment $\boldsymbol{c}$ and unique (subject-specific) environment $\boldsymbol{e}$, and their covariance structures take the following forms:

$$\boldsymbol{g} \sim \mathrm{N}(\boldsymbol{0}, \sigma_A^2\boldsymbol{K}), \quad \boldsymbol{c} \sim \mathrm{N}(\boldsymbol{0}, \sigma_C^2\boldsymbol{\Lambda}), \quad \boldsymbol{e} \sim \mathrm{N}(\boldsymbol{0}, \sigma_E^2\boldsymbol{I}_m), \qquad [2]$$

where σ_A^2, σ_C^2, and σ_E^2 are the additive genetic variance, common environmental variance, and unique environmental variance, respectively; $\boldsymbol{K}$ is

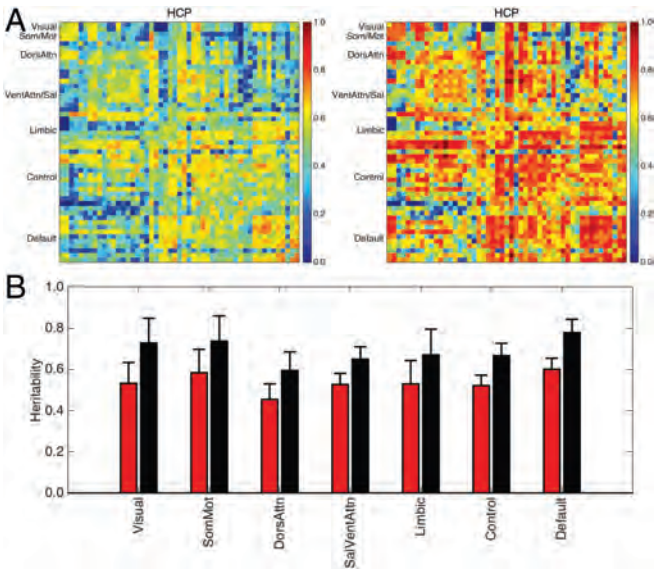

Fig. 3. Heritability of functional connectivity measurements. (*A*) Conventional heritability estimates of functional connectivity measurements computed by averaging repeat measurements for each subject and applying the classical ACE model (*Left*) and the heritability estimates of the stable, nontransient component of functional connectivity computed using the proposed model (*Right*). (*B*) Average of the heritability estimates of within-network functional connectivity measurements for each of the seven functional networks. Heritability was estimated using the proposed method (black) and the classical ACE model (red). The standard errors shown were estimated by a block-jackknife procedure.

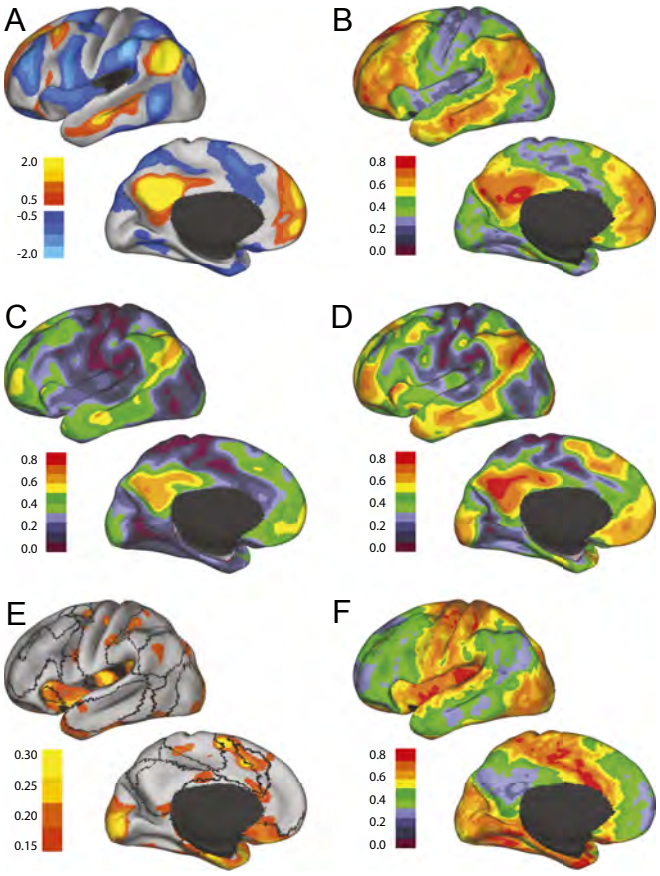

Fig. 4. Analysis of the functional connectivity profile seeded at PCC in the HCP sample. (*A*) Average functional connectivity profile across subjects. (*B*) Test–retest reliability of the functional connectivity profile. (*C*) Heritability estimates of the connectivity profile computed using the classical ACE model. (*D*) Heritability estimates of the stable, nontransient component of the connectivity profile computed using the proposed method. (*E*) Difference of the heritability estimates computed by the proposed model and the classical ACE model, with the boundaries of the seven functional networks overlaid. (*F*) Proportion of the total phenotypic variation attributable to intrasubject variation.

an $m \times m$ genetic similarity matrix, $\boldsymbol{\Lambda}$ is an $m \times m$ matrix that quantifies shared environment between pairs of individuals, and $\boldsymbol{I}_m$ is an $m \times m$ identity matrix. In familial studies, $\boldsymbol{K}$ is twice the kinship matrix. The ij-th entry of the kinship matrix, ϕ_{ij}, defines genetic relatedness for subjects i and j, and in general can be derived from pedigree information. $\boldsymbol{\Lambda}$ usually reflects household sharing between pairs of individuals. In the present study, $\phi_{ij} = 1/2$ for monozygotic (MZ) twins and $\phi_{ij} = 1/4$ for dizygotic (DZ) twins and full siblings, and we assume that subjects that have the same parents share the same environment and the corresponding elements in $\boldsymbol{\Lambda}$ are one. We further assume that $\epsilon_{ij} \sim \mathrm{N}(0, \sigma_M^2)$.

Using matrix notations $\boldsymbol{y}_i = [y_{i1}, \cdots, y_{in_i}]^\top$, $\boldsymbol{X}_i = [\boldsymbol{x}_{i1}, \cdots, \boldsymbol{x}_{in_i}]^\top$, $\boldsymbol{\epsilon}_i = [\epsilon_{i1}, \cdots, \epsilon_{in_i}]^\top$, and denoting $\mathbf{1}_{n_i}$ as a column vector of n_i ones, model **1** can be written as

$$\boldsymbol{y}_i = \boldsymbol{X}_i\beta + \mathbf{1}_{n_i}\gamma_i + \boldsymbol{\epsilon}_i, \quad i = 1, 2, \cdots, m. \qquad [3]$$

We can further stack the data from all subjects and write model **3** as

$$\boldsymbol{y} = \boldsymbol{X}\beta + \boldsymbol{T}\boldsymbol{\gamma} + \boldsymbol{\epsilon}, \quad \boldsymbol{\gamma} = \boldsymbol{g} + \boldsymbol{c} + \boldsymbol{e}, \qquad [4]$$

where $\boldsymbol{y} = [\boldsymbol{y}_1^\top, \cdots, \boldsymbol{y}_m^\top]^\top$, $\boldsymbol{X} = [\boldsymbol{X}_1^\top, \cdots, \boldsymbol{X}_m^\top]^\top$, $\boldsymbol{T} = \mathrm{blkdiag}\{\mathbf{1}_{n_1}, \cdots, \mathbf{1}_{n_m}\}$ is a block diagonal matrix of size $n \times m$, $n = \sum_{i=1}^m n_i$ is the total number of measurements, and $\boldsymbol{\epsilon} = [\boldsymbol{\epsilon}_1^\top, \cdots, \boldsymbol{\epsilon}_m^\top]^\top$. The covariance matrix of $\boldsymbol{y}$ can be calculated as

$$\mathbf{cov}[\boldsymbol{y}] = \boldsymbol{T}\mathbf{cov}[\gamma]\boldsymbol{T}^\top + \mathbf{cov}[\boldsymbol{\epsilon}] = \sigma_A^2\boldsymbol{T}\boldsymbol{K}\boldsymbol{T}^\top + \sigma_C^2\boldsymbol{T}\boldsymbol{\Lambda}\boldsymbol{T}^\top + \sigma_E^2\boldsymbol{T}\boldsymbol{T}^\top + \sigma_M^2\boldsymbol{I}_n. \qquad [5]$$

We then define the nontransient heritability of a trait as the proportion of the total stable, nontransient intersubject variation that can be explained by genetic variation in the population:

$$h^2 = \frac{\sigma_A^2}{\sigma_A^2 + \sigma_C^2 + \sigma_E^2}. \qquad [6]$$

Unbiased estimates of the unknown variance component parameters σ_A^2, σ_C^2, σ_E^2, and σ_M^2 can be obtained using the ReML algorithm (22).

We note that when no repeat measurement is available, that is, $n_i = 1$ for all i, we have $n = m$, $\boldsymbol{T} = \boldsymbol{I}_m$, and the model specified in Eqs. **4** and **5** becomes unidentifiable. In this case, $\boldsymbol{e}$ and ϵ cannot be distinguished and have to be combined, leading to the classical ACE model and the classical definition of heritability. With repeat measurements, however, $\boldsymbol{e}$ and ϵ have different covariance structures and thus can be modeled separately.

The HCP. The HCP collects imaging, behavioral, and demographic data from a large population of young and healthy adults. Here we analyzed 582 non-Hispanic/Latino European subjects (22 to 36 y of age) collected by the WU-Minn HCP Consortium. These subjects (age, 29.21 ± 3.47 y; female, 55.84%) come from 248 families and comprise 92 MZ twin pairs, 46 DZ twin pairs, 250 full siblings, and 56 singletons (single-birth individuals without siblings). Further details about the recruitment process and imaging data acquisition can be found in refs. 17 and 32–34.

The Brain GSP. The Harvard/MGH Brain GSP is a neuroimaging and genetics study of brain and behavioral phenotypes. Here we analyzed 809 unrelated young adults (18 to 35 y of age) of non-Hispanic European ancestry with no history of psychiatric illnesses or major health problems (age, 20.84 ± 2.77 y; female, 55.25%; right-handedness, 88.38%). The study was approved by the Partners Health Care IRB and the Harvard University Committee on the Use of Human Subjects in Research. All participants provided written informed consent in accordance with guidelines set by the IRB. For further details about the recruitment process, participants, and imaging data acquisition, we refer the reader to refs. 18 and 19.

Preprocessing of rs-fMRI Data. We used MSM-All [areal feature-based Multimodal Surface Matching algorithm (35)] registered and ICA+FIX [FMRIB's ICA-based X-noiseifier (36)] denoised rs-fMRI data distributed by the HCP. Among the 582 subjects we analyzed, 555 subjects had two rs-fMRI sessions on separate days and 27 subjects had one rs-fMRI session. Each rs-fMRI session consists of two scans of ∼15 min each with alternate phase encoding directions (left to right and right to left, respectively). For each scan, we smoothed the MSM-All registered and FIX denoised time series using a surface-based Gaussian kernel with 6-mm FWHM and resampled the data to FreeSurfer's fsaverage5 representation, which consists of $n_{\mathrm{vtx}} = 20{,}484$ vertices across the two hemispheres. For each rs-fMRI session, we then temporally standardized (subtracted the mean and divided by SD) and concatenated the two scans.

The preprocessing of the GSP data followed the procedures outlined in ref. 18. All 809 GSP subjects had two rs-fMRI scans of approximately 6 min each, acquired on the same model 12-channel head coil. Both scans had slice-based temporal signal-to-noise ratio greater than 100. We spatially smoothed each scan using a surface-based Gaussian kernel with 6-mm FWHM and resampled the time series to fsaverage5.

Computation of Functional Connectivity. For each HCP session and GSP scan we computed an $n_{\mathrm{vtx}} \times n_{\mathrm{vtx}}$ Pearson correlation coefficient matrix using the preprocessed time series. The correlation coefficients were then spatially standardized into z-scores to make functional connectivity strength between each pair of vertices comparable across subjects. The rs-fMRI–based seven-network parcellation of the cortex obtained in ref. 18 was split into 51 spatially contiguous regions across the two hemispheres, and the z-scores were averaged within and across network regions into a 51 × 51 matrix.

Test–Retest Reliability. In the HCP sample, test–retest reliability of the network-level functional connectivity measurements (i.e., each average z-score in the 51 × 51 matrix) was computed as the Pearson correlation coefficient of z-scores from 247 unrelated subjects who were sampled from different families and had repeat rs-fMRI sessions. In the GSP sample, test–retest reliability was computed similarly using all of the 809 subjects.

Heritability Analysis. We estimated the nontransient heritability of each rs-fMRI–derived functional connectivity measurement in the 51 × 51 matrix in the HCP sample using our proposed LME model as specified in Eqs. **4** and **5**

and the definition of heritability in Eq. **6**, adjusting for age, sex, and handedness as fixed-effect covariates. To benchmark our results, for each entry in the 51×51 matrix we averaged measurements from repeat sessions to obtain one scalar measurement for each subject and then estimated the heritability using the classical ACE model, adjusting for the same covariates.

We averaged heritability estimates of within-network functional connectivity measurements to obtain an overall heritability estimate for each of the seven functional networks. To estimate the variance of the overall heritability estimate we used a block-jackknife procedure whereby each time one family was left out and the overall heritability was reestimated using the subsample. This procedure was repeated for all of the $n_{\text{fam}} = 248$ families to yield the jackknife heritability estimates $\widehat{h}^2_k$, $k = 1, 2, \cdots, n_{\text{fam}}$. The variance of the overall heritability estimate was then estimated as in ref. 37:

$$\mathbf{var}\left[\widehat{h}^2\right] = \frac{n_{\text{fam}} - 1}{n_{\text{fam}}} \sum_{k=1}^{n_{\text{fam}}} \left(\widehat{h}^2_k - \widehat{h}^2_\bullet\right)^2, \qquad [7]$$

where $\widehat{h}^2_\bullet = \sum_{k=1}^{n_{\text{fam}}} \widehat{h}^2_k / n_{\text{fam}}$.

Analysis of the PCC Seed Map. We used the MNI coordinates -3, -49, 25 reported in ref. 18 as the seed location in PCC and found the vertex (MNI coordinates -2.917, -48.487, 24.970) in the fsaverage5 system that has the shortest Euclidean distance to the seed. For each subject, the row in the $n_{\text{vtx}} \times n_{\text{vtx}}$ spatially standardized correlation coefficient matrix that corresponds to the selected vertex was then used as the functional connectivity profile of PCC. The classical ACE model and the proposed LME model were used to estimate the heritability for each of the elements in the functional connectivity profile in the HCP sample. Surface maps of the heritability estimates were smoothed using a Gaussian kernel with 12-mm FWHM before visualization.

ACKNOWLEDGMENTS. The authors would like to thank B. T. Thomas Yeo for providing the 51 spatial components of the seven-network parcellation of the cortex. Twenty individual investigators at Harvard and MGH generously contributed data to the overall project. This research used resources provided by the Center for Functional Neuroimaging Technologies and a P41 Biotechnology Resource Grant (P41EB015896) supported by the NIH. This work also involved the use of instrumentation supported by the NIH Shared Instrumentation Grant Program (S10RR023043 and S10RR023401). Data were provided in part by the WU-Minn HCP Consortium (principal investigators: David Van Essen and Kamil Ugurbil; Grant 1U54MH091657) funded by the 16 NIH Institutes and Centers that support the NIH Blueprint for Neuroscience Research and by the McDonnell Center for Systems Neuroscience at Washington University. Data were also provided in part by the Brain GSP of Harvard University and MGH, with support from the Center for Brain Science Neuroinformatics Research Group, Athinoula A. Martinos Center for Biomedical Imaging, Center for Human Genetic Research, and Stanley Center for Psychiatric Research. This research was also funded in part by NIH Grants R01NS083534, R01NS070963, K25EB013649, R21AG050122, and R41AG052246 (to M.R.S.); K24MH094614 and R01MH101486 (to J.W.S.); K01MH099232 (to A.J.H.); an MGH ECOR interim support fund (to M.R.S.); and an MGH ECOR Tosteson postdoctoral fellowship award (to T.G.). J.W.S. is a Tepper Family MGH Research Scholar and was also supported in part by a gift from the Demarest Lloyd, Jr. Foundation.

1. Visscher P, Hill W, Wray N (2008) Heritability in the genomics era—Concepts and misconceptions. *Nat Rev Genet* 9:255–266.
2. Falconer D (1960) *Introduction to Quantitative Genetics* (Oliver and Boyd, Edinburgh).
3. Almasy L, Blangero J (1998) Multipoint quantitative-trait linkage analysis in general pedigrees. *Am J Hum Genet* 62:1198–1211.
4. Polderman T, et al. (2015) Meta-analysis of the heritability of human traits based on fifty years of twin studies. *Nat Genet* 47:702–709.
5. Yang J, et al. (2010) Common SNPs explain a large proportion of the heritability for human height. *Nature Genetics* 42:565–569.
6. Yang J, Lee S, Goddard M, Visscher P (2011) GCTA: A tool for genome-wide complex trait analysis. *Am J Hum Genet* 88:76–82.
7. Golan D, Lander E, Rosset S (2014) Measuring missing heritability: Inferring the contribution of common variants. *Proc Natl Acad Sci USA* 111:E5272–E5281.
8. Ge T, et al. (2015) Massively expedited genome-wide heritability analysis (MEGHA). *Proc Natl Acad Sci USA* 112:2479–2484.
9. Ge T, et al. (2016) Multidimensional heritability analysis of neuroanatomical shape. *Nat Commun* 7:13291.
10. Krüger G, Glover G (2001) Physiological noise in oxygenation-sensitive magnetic resonance imaging. *Magn Reson Med* 46:631–637.
11. Triantafyllou C, et al. (2005) Comparison of physiological noise at 1.5 T, 3 T and 7 T and optimization of fMRI acquisition parameters. *Neuroimage* 26:243–250.
12. Hutchison R, et al. (2013) Dynamic functional connectivity: Promise, issues, and interpretations. *Neuroimage* 80:360–378.
13. Mueller S, et al. (2013) Individual variability in functional connectivity architecture of the human brain. *Neuron* 77:586–595.
14. Glahn D, et al. (2010) Genetic control over the resting brain. *Proc Natl Acad Sci USA* 107:1223–1228.
15. Fornito A, et al. (2011) Genetic influences on cost-efficient organization of human cortical functional networks. *J Neurosci* 31:3261–3270.
16. Thompson P, Ge T, Glahn D, Jahanshad N, Nichols T (2013) Genetics of the connectome. *Neuroimage* 80:475–488.
17. Van Essen D, et al. (2013) The WU-Minn human connectome project: An overview. *Neuroimage* 80:62–79.
18. Yeo B, et al. (2011) The organization of the human cerebral cortex estimated by intrinsic functional connectivity. *J Neurophysiol* 106:1125–1165.
19. Holmes A, et al. (2015) Brain Genomics Superstruct Project initial data release with structural, functional, and behavioral measures. *Sci Data* 2:150031.
20. Laird N, Ware J (1982) Random-effects models for longitudinal data. *Biometrics* 38:963–974.
21. Verbeke G, Molenberghs G (2009) *Linear Mixed Models for Longitudinal Data* (Springer, New York).
22. Patterson H, Thompson R (1971) Recovery of inter-block information when block sizes are unequal. *Biometrika* 58:545–554.
23. Kendler K, Karkowski L, Prescott C (1999) Fears and phobias: Reliability and heritability. *Psychol Med* 29:539–553.
24. Dohm M (2002) Repeatability estimates do not always set an upper limit to heritability. *Funct Ecol* 16:273–280.
25. Deichmann R, Gottfried J, Hutton C, Turner R (2003) Optimized EPI for fMRI studies of the orbitofrontal cortex. *Neuroimage* 19:430–441.
26. Weiskopf N, Hutton C, Josephs O, Deichmann R (2006) Optimal EPI parameters for reduction of susceptibility-induced BOLD sensitivity losses: A whole-brain analysis at 3 T and 1.5 T. *Neuroimage* 33:493–504.
27. Power J, Barnes K, Snyder A, Schlaggar B, Petersen S (2012) Spurious but systematic correlations in functional connectivity MRI networks arise from subject motion. *Neuroimage* 59:2142–2154.
28. Van Dijk K, Sabuncu M, Buckner R (2012) The influence of head motion on intrinsic functional connectivity MRI. *Neuroimage* 59:431–438.
29. Satterthwaite T, et al. (2012) Impact of in-scanner head motion on multiple measures of functional connectivity: Relevance for studies of neurodevelopment in youth. *Neuroimage* 60:623–632.
30. van den Heuvel M, et al. (2013) Genetic control of functional brain network efficiency in children. *Eur Neuropsychopharmacol* 23:19–23.
31. Buckner R, Andrews-Hanna J, Schacter D (2008) The brain's default network. *Ann N Y Acad Sci* 1124:1–38.
32. Van Essen D, et al. (2012) The Human Connectome Project: A data acquisition perspective. *Neuroimage* 62:2222–2231.
33. Smith S, et al. (2013) Resting-state fMRI in the human connectome project. *Neuroimage* 80:144–168.
34. Glasser M, et al. (2013) The minimal preprocessing pipelines for the Human Connectome Project. *Neuroimage* 80:105–124.
35. Robinson E, et al. (2014) MSM: A new flexible framework for Multimodal Surface Matching. *Neuroimage* 100:414–426.
36. Salimi-Khorshidi G, et al. (2014) Automatic denoising of functional MRI data: Combining independent component analysis and hierarchical fusion of classifiers. *Neuroimage* 90:449–468.
37. Efron B, Tibshirani R (1994) *An Introduction to the Bootstrap* (CRC, Boca Raton, FL).